



Resistivity and heat transfer characteristics of high temperature film anemometers  
by Scott Gerald Anders

A thesis submitted in partial fulfillment of the requirements for the degree of Master of Science  
Mechanical Engineering  
Montana State University  
© Copyright by Scott Gerald Anders (1990)

Abstract:

The resistivity and heat transfer characteristics of a wedge-shaped high temperature film anemometer probe are studied here. These film anemometers were designed specifically for flows with stagnation temperatures up to 760 C and dynamic pressures of around 20 psia. The necessary theory was first developed from low speed applications of film anemometers and from hot-wire theory. The proper calibration equipment and procedures were selected so that the required raw data could be collected. The theory was used to reduce the data to the variables of interest. Oven calibration data were taken for the temperature range 20 C to 500 C. The resulting data were fit with a second degree polynomial in order to give the correct reference resistance and resistivity coefficients which were unique for each probe. Flow data were taken for Mach numbers 0, 0.5, 1, 2, and 3. Data for Mach 0.5, 1, 2, and 3 were taken at stagnation temperatures of 15 C and 65 C. The resulting dimensional Reynolds number range covered by these various flows was from zero to 120,000 1/cm. Small amounts of data were also collected at Mach 6 and Mach 8. For the flows investigated the Nusselt number was found to be a function of the square root of the Reynolds number with no apparent Mach number dependence. In order to obtain this Nusselt number the measured Nusselt number must be corrected for its conduction contribution as the developed theory indicates. The temperature recovery factor was found to have a maximum at a value of approximately one and it was found to decrease with increasing Mach number to a minimum of about .8 at Mach 8. It also exhibited a Reynolds number dependence for Mach numbers of 3 and higher.

**RESISTIVITY AND HEAT TRANSFER CHARACTERISTICS  
OF HIGH TEMPERATURE FILM ANEMOMETERS**

by

Scott Gerald Anders

A thesis submitted in partial fulfillment  
of the requirements for the degree

of

Master of Science

in

Mechanical Engineering

**MONTANA STATE UNIVERSITY**  
Bozeman, Montana

May 1990

N378  
AN 206

**APPROVAL**

of a thesis submitted by  
  
Scott Gerald Anders

This thesis has been read by each member of the thesis committee and has been found to be satisfactory regarding content, English usage, format, citations, bibliographic style, and consistency, and is ready for submission to the College of Graduate Studies.

5/15/90  
Date

A. K. Kmetz  
Chairperson, Graduate Committee

Approved for the Major Department

5/15/90  
Date

H. E. Larsen  
Head, Major Department

Approved for the College of Graduate Studies

May 25, 1990  
Date

Henry L. Parsons  
Graduate Dean

**STATEMENT OF PERMISSION TO USE**

In presenting this thesis in partial fulfillment of the requirements for a master's degree at Montana State University, I agree that the Library shall make it available to borrowers under rules of the Library. Brief quotations from this thesis are allowable without special permission, provided that accurate acknowledgment of source is made.

Permission for extensive quotation from or reproduction of this thesis may be granted by my major professor, or in his absence, by the Dean of Libraries when, in the opinion of either, the proposed use of the material is for scholarly purposes. Any copying or use of the material in this thesis for financial gain shall not be allowed without my written permission.

Signature Scott G. Anderson

Date 5/15/90

## ACKNOWLEDGMENTS

The author is indebted to the following persons for their contributions to this investigation:

His advisor, Dr. Anthony Demetriades, for his guidance throughout this investigation.

John Rompel, for designing and constructing the special electronic equipment used in this investigation.

Pat Vowell, for his assistance in constructing or repairing the equipment used in this investigation.

Dr. Alan George and Dr. Richard Rosa for their support as committee members.

The Mechanical Engineering Department of Montana State University for financial assistance.

The Calspan Corporation, AEDC operations, for consultations regarding hot-film data.

Rene' Tritz, for typing and checking the final version of this thesis.

## TABLE OF CONTENTS

	<u>Page</u>
LIST OF TABLES . . . . .	vii
LIST OF FIGURES . . . . .	viii
NOMENCLATURE . . . . .	xii
ABSTRACT . . . . .	xv
1. INTRODUCTION . . . . .	1
2. FILM ANEMOMETER PRINCIPLE AND RESEARCH GOALS . . . . .	4
3. HEAT BALANCE FOR THERMAL SENSORS . . . . .	6
Cylinder With No Conduction Loss . . . . .	6
Cylinder With Conduction Loss . . . . .	7
Film Anemometer With No Substrate . . . . .	9
Film Anemometer With Substrate . . . . .	10
General Heat Balance Equation . . . . .	14
4. THEORY OF MEASUREMENT . . . . .	16
Resistance-Temperature Relations . . . . .	16
Nusselt Number Dependence On Power . . . . .	18
Conduction Term Correction . . . . .	22
5. HEAT TRANSFER FROM STAGNATION POINT SENSORS . . . . .	26
6. EXPERIMENTAL APPARATUS . . . . .	31
Film Anemometer Probes . . . . .	31
Programmable Current Supply (PCS) . . . . .	33
Oven Calibration Hardware . . . . .	35
Low Velocity Tunnel (LVT) . . . . .	38
Supersonic Wind Tunnel (SWT) . . . . .	42

**TABLE OF CONTENTS—Continued**

	<u>Page</u>
7. CALIBRATION PROCEDURES . . . . .	48
Oven Calibration Procedures . . . . .	48
Flow Calibration Procedures . . . . .	51
8. RESULTS . . . . .	53
Temperature Endurance and Stability . . . . .	53
Dynamic Pressure Endurance . . . . .	55
Resistance and Resistivity Coefficients . . . . .	56
Dependence of The Nusselt Number On Power . . . . .	62
Temperature Recovery Factor Dependence on Flow Properties . . . . .	66
Nusselt Number Dependence On Flow Properties . . . . .	73
9. CONCLUSIONS . . . . .	91
Theoretical Conclusions . . . . .	91
Experimental Conclusions . . . . .	93
APPENDICES . . . . .	96
Appendix A — RADIATION LOSS FROM FILM ANEMOMETER . . . . .	97
Appendix B — CONVECTION LOSS IN CALIBRATION OVEN . . . . .	100
Appendix C — NEWOVEN PROGRAM . . . . .	103
Appendix D — FLOWRDCT PROGRAM . . . . .	116
REFERENCES CITED . . . . .	128

LIST OF TABLES

<u>Table</u>	<u>Page</u>
1. Resistivity Coefficients for 39 Oven Calibrations . . . . .	57



## LIST OF FIGURES

<u>Figure</u>	<u>Page</u>
1. One-Dimensional Model for Heat Loss to Substrate . . . . .	12
2. Approximation of Distance $L$ for "Thin-Rod" Model . . . . .	13
3. Film Resistance Dependence on Power Fit with a Second Degree Polynomial . . . . .	19
4. Hypothetical Case of Measured Nusselt Number Dependence on Flow Properties . . . . .	25
5. Hypothetical Case of "Actual" Nusselt Number Dependence on Flow Properties . . . . .	25
6. Local Heat Transfer Rate from the Surface of a Hemisphere in Hypersonic Flow . . . . .	29
7. Correlation of Hot-Wire Heat Transfer at Low Reynolds Numbers. Nusselt and Reynolds Number Evaluated at Stagnation Temperature . . . . .	30
8. Film Probe Design . . . . .	32
9. System Components Used to Collect Raw Data . . . . .	34
10. Top Cut-Away View of Oven Calibration Hardware with Probe in Place . . . . .	36
11. Probe and Accompanying Thermocouple in Probe Holder . . . . .	37
12. Low Velocity Tunnel . . . . .	39
13. Probe Holder for Low Velocity Tunnel . . . . .	40
14. Calibration Results of Low Velocity Tunnel . . . . .	41

**LIST OF FIGURES—Continued**

<u>Figure</u>	<u>Page</u>
15. General Circuit of Supersonic Wind Tunnel . . . . .	44
16. Transducer Calibration for Measurement of Pitot Pressure in Supersonic Wind Tunnel . . . . .	45
17. Supersonic Wind Tunnel Film Probe Holder with Accompanying Pitot Probe . . . . .	46
18. Mach Number Variation With Position . . . . .	47
19. Summarized Output for Oven Calibration For Probe Number 50 . . . . .	50
20. Graphical Presentation of Oven Calibration Results for Probe 48 . . . . .	58
21. Temperature Recovery Factor Variation for a Typical Probe. Resistivity Calibration with $\beta = 0$ . Resistance versus Power Data Fit with a Second Degree Polynomial . . . . .	59
22. Temperature Recovery Factor Variation for a Typical Probe. Resistivity Calibration with $\beta \neq 0$ . Resistance versus Power Data Fit with a Second Degree Polynomial . . . . .	60
23. Heat Transfer Characteristics for a Typical Probe. Resistance versus Power Data Fit with a Second Degree Polynomial . . . . .	61
24. Characteristics of the Constant $D$ for Probe 48 . . . . .	63
25. Characteristics of the Constant $D$ for Probe 50 . . . . .	64
26. Characteristics of the Constant $D$ for Probe 56 . . . . .	65
27. Temperature Recovery Factor Dependence on Flow Properties for Probe 48 . . . . .	68

LIST OF FIGURES—Continued

<u>Figure</u>	<u>Page</u>
28. Temperature Recovery Factor Dependence on Flow Properties for Probe 50 . . . . .	69
29. Temperature Recovery Factor Dependence on Flow Properties for Probe 56 . . . . .	70
30. Measured Nusselt Number Characteristics in a Mach 8 Flow . . . . .	71
31. Temperature Recovery Factor Dependence in a Mach 8 Flow . . . . .	71
32. Normalized Temperature Recovery Factor Variation with Mach Number . . . . .	72
33. Measured Nusselt Number Characteristics for Probe 48 . . . . .	74
34. Measured Nusselt Number Characteristics for Probe 50 . . . . .	75
35. Measured Nusselt Number Characteristics for Probe 56 . . . . .	76
36. Measured Nusselt Number Characteristics for Probe 48 in Terms of the Square Root of the Reynolds Number . . . . .	77
37. Measured Nusselt Number Characteristics for Probe 50 in Terms of the Square Root of the Reynolds Number . . . . .	78
38. Measured Nusselt Number Characteristics for Probe 56 in Terms of the Square Root of the Reynolds Number . . . . .	79
39. Measured Nusselt Number Dependence on the Inverse Square Root of the Thermal Conductivity in the Absence of Forced Convection . . . . .	80
40. Temperature Dependence of the Measured Nusselt Number in the Absence of Forced Convection . . . . .	81
41. Convective Nusselt Number Characteristics for Probe 48 . . . . .	82
42. Convective Nusselt Number Characteristics for Probe 50 . . . . .	83

LIST OF FIGURES—Continued

<u>Figure</u>	<u>Page</u>
43. Convective Nusselt Number Characteristics for Probe 56 . . . . .	84
44. Measured Nusselt Number Characteristics for Probe 50. Nusselt Number Evaluated at the Stagnation Temperature. Reynolds Number Evaluated at the Free-Stream Temperature . . . . .	87
45. Measured Nusselt Number Characteristics for Probe 50. Nusselt Number Evaluated at the Recovery Temperature. Reynolds Number Evaluated at the Free-Stream Temperature . . . . .	88
46. Measured Nusselt Number Characteristics for Probe 50. Nusselt Number Evaluated at the Stagnation Temperature. Reynolds Number Evaluated at the Stagnation Temperature . . . . .	89
47. Measured Nusselt Number Characteristics for Probe 50. Nusselt Number Evaluated at the Recovery Temperature. Reynolds Number Evaluated at the Stagnation Temperature . . . . .	90
48. NEWOVEN Program . . . . .	104
49. FLWRDCT Program . . . . .	117

## NOMENCLATURE

<u>Symbol</u>	<u>Description</u>
$A$	Cross sectional area
$A_s$	Surface area
$c$	Constant
$d$	Diameter
$G$	Grashof number
$g$	Gravitational constant
$h$	Convective heat transfer coefficient
$i$	Current
$k$	Thermal conductivity
$L_c$	Conduction loss term
$l$	Length of sensor
LVT	Low velocity tunnel
$M$	Mach number
$N$	Nusselt number
$N_{cnd}$	Conduction contribution to measured Nusselt number
$N_m$	Measured Nusselt number
$P$	Perimeter
PCS	Programmable Current Supply
$Pr$	Prandtl number

## NOMENCLATURE—Continued

<u>Symbol</u>	<u>Description</u>
$Q_{rad}$	Heat transfer due to radiation
$q$	Heat transfer rate
$R$	Resistance
$R_C$	Resistance of cable connecting probe to current supply
$R_{LW}$	Resistance of platinum wire leads
$R_T$	Total line resistance
$Re$	Reynolds number
$r$	Radius
SWT	Supersonic wind tunnel
$T$	Temperature
$V$	Velocity
$W$	Power
$y$	Differential height of manometer
$\alpha$	First coefficient of resistivity
$\beta$	Second coefficient of resistivity
$\gamma$	Specific weight
$\epsilon$	Emissivity
$\eta$	Temperature recovery factor
$\xi$	Third coefficient of resistivity
$\sigma$	Stefan-Boltzmann constant
$\tau$	Temperature loading factor

NOMENCLATURE-Continued

<u>Symbol</u>	<u>Description</u>
( ) <sub>e</sub>	At recovery temperature
( ) <sub>f</sub>	Based on film
( ) <sub>r</sub>	At reference condition (0 C)
( ) <sub>s</sub>	At supports
( ) <sub>w</sub>	Based on wire
( ) <sub>∞</sub>	At free-stream temperature

## ABSTRACT

The resistivity and heat transfer characteristics of a wedge-shaped high temperature film anemometer probe are studied here. These film anemometers were designed specifically for flows with stagnation temperatures up to 760 C and dynamic pressures of around 20 psia. The necessary theory was first developed from low speed applications of film anemometers and from hot-wire theory. The proper calibration equipment and procedures were selected so that the required raw data could be collected. The theory was used to reduce the data to the variables of interest. Oven calibration data were taken for the temperature range 20 C to 500 C. The resulting data were fit with a second degree polynomial in order to give the correct reference resistance and resistivity coefficients which were unique for each probe. Flow data were taken for Mach numbers 0, 0.5, 1, 2, and 3. Data for Mach 0.5, 1, 2, and 3 were taken at stagnation temperatures of 15 C and 65 C. The resulting dimensional Reynolds number range covered by these various flows was from zero to 120,000 1/cm. Small amounts of data were also collected at Mach 6 and Mach 8. For the flows investigated the Nusselt number was found to be a function of the square root of the Reynolds number with no apparent Mach number dependence. In order to obtain this Nusselt number the measured Nusselt number must be corrected for its conduction contribution as the developed theory indicates. The temperature recovery factor was found to have a maximum at a value of approximately one and it was found to decrease with increasing Mach number to a minimum of about .8 at Mach 8. It also exhibited a Reynolds number dependence for Mach numbers of 3 and higher.



## CHAPTER 1

### INTRODUCTION

As the area of supersonic and hypersonic research expands, the need for improved instrumentation to measure both mean flow properties and turbulent fluctuations becomes increasingly important. The majority of information in the area of turbulence fluctuation measurement has been gathered by the hot-wire anemometer. The hot-wire consists of a very fine wire mounted perpendicular to the flow on two small supports. By monitoring the resistance and power dissipation of the wire, the recovery temperature and the Nusselt number can be determined. If these are then investigated for different flow regimes their dependence on Mach number, Reynolds number, and temperature can be determined. These dependencies can then be used in the measurement of turbulent fluctuations. Further discussion on the hot-wire method can be found in References [1-4].

Though hot-wires have proven themselves useful, they are limited to flows where the temperatures and dynamic pressures are moderate. They also retain some undesirable characteristics such as a Mach number dependence at low Reynolds numbers due to restrictions on spatial resolution. Since high Mach number and high dynamic pressure facilities are usually small in order to be economically justifiable, the areas of interest in a particular flow to be studied require instrumentation that has high spatial resolution. A high spatial resolution is also

required if high turbulence frequencies (responses of around 300 kHz) are going to be measured. These requirements in turn put limitations on the magnitude of hot-wire diameters. These small diameter wires bring the instrument into the low Reynolds number range where the Nusselt number becomes Mach number dependent. Also, when flow dynamic pressures or stagnation temperatures become high the mechanical strength of the hot-wire is found insufficient to prevent wire breakage. To make the situation even more severe, many facilities are not adequately filtered to remove tiny particles which can destroy the small unsupported wire. These requirements for a high structural endurance, high frequency response, and high spatial resolution have given rise to the film anemometer probe.

Film anemometer probes have been used in the past mainly for measurement in liquids such as water and blood where hot-wires would be impractical [2,5,6]. The use of a film anemometer probe in a supersonic flow has received limited attention however, resulting in limited sources on their calibration methods, resistivity, and heat transfer characteristics. Now that more severe requirements have been placed on this type of instrumentation, use of the film anemometer has become more promising and the need for knowing its characteristics increasingly important. The requirements for the film anemometer probes investigated here were that the probes must be able to be used for high temperature (760 C), high dynamic pressure flows [7]. For these probes, the films are deposited on the stagnation line of a wedge-shaped probe tip. This film, being supported by the hard probe body tip, is much less subject to failure due to mechanical stresses as compared to the hot-wire yet still will be able to maintain the required frequency response and spatial resolution.

The theory developed for the films is drawn from low speed applications of film anemometers and from hot-wire anemometer theory which shares many points of

similarity. Much of the theory has also been previously established by Ling [8] and Demetriades [7]. The calibration methods used here are developed on the basis of this theory, the results of which show that the heat transfer characteristics of hot-films are quite similar to hot-wires. The most noticeable deviation is the large conduction loss to the substrate for the film.

Much time was spent investigating the hot-film probe resistivity and heat transfer characteristics since they must be understood in order to move on to the measurement of turbulence fluctuations. In order to make proper measurement of turbulence one must know accurately: the resistance and resistivity coefficients; the temperature recovery factor dependence on Mach number, stagnation temperature, Reynolds number; and the Nusselt number dependence on Mach number, stagnation temperature, Reynolds number, and temperature loading (power). The following is an account of how all of these are determined and the results of each. For information on the use of these characteristics for turbulent flow measurements see Demetriades [9].

## CHAPTER 2

### FILM ANEMOMETER PRINCIPLE AND RESEARCH GOALS

The principle of operation of the hot-film anemometer probe is the following: If an object is placed in a moving medium and then heated, heat will be exchanged between the object and the medium. The rate at which the heat is exchanged depends on the characteristics of the object, the physical characteristics of the medium, and the flow characteristics of the medium. The heat is introduced by a constant electrical current and the corresponding resistance of the object is monitored. By first observing and recording the behavior of the object for a variety of flow conditions, the object can later be used to determine unknown flow characteristics. This is the general method described and used by Laufer and McClellan [10].

The two aims of this research were to determine (a) the resistivity characteristics and (b) the heat transfer characteristics for film anemometers designed for high temperature hypersonic research. These film anemometers were designed to be able to withstand continuous exposure to 760 C stagnation temperatures and dynamic pressure loads exceeding 140 kPa (20 psia). This placed serious restrictions on probe design and development. Despite the design problems the two aims of this research were carried out while the probes were being developed. The determination of the resistance and resistivity characteristics included selection of the proper calibration equipment and procedures and the determination of the proper handling of the calibration data. The determination of the heat transfer

characteristics of the film anemometer probe also included selection of the proper calibration equipment, procedures and data handling. In addition to these the second aim included determination of the proper theory of measurement, relating the film anemometer probe electrical output to flow dependence variables by theory, and relating these variables to the flow characteristics such as the temperature recovery factor, Reynolds number, Mach number, and flow temperature.

## CHAPTER 3

## HEAT BALANCE FOR THERMAL SENSORS

As briefly mentioned in Chapter 2, the rate at which heat is exchanged from the object to the medium depends on the characteristics of the object, the physical characteristics of the medium, and the flow characteristics of the medium. In order to measure these flow characteristics by the method described, the rate at which heat is exchanged to the medium must be known. This requires analysis of the heat loss for the object of interest. The approach taken here is to start with the simplest model and work towards the desired but more complicated model.

Cylinder With No Conduction Loss

An electrically heated cylinder in a cross flow with no end losses can lose heat only by radiation and convection. If it is assumed that radiation losses are negligible the power balance is

$$(1) \quad i^2 R = hA_s (T - T_\infty)$$

where

$i^2 R$  = power input

$h$  = convective heat transfer coefficient

$A_s$  = surface area

$T$  = temperature of film

$T_\infty$  = temperature of surroundings

See pages xii–xiv for list of nomenclature used throughout the text. For a cylinder immersed in a compressible flow the temperature of the fluid nearest the sensor will not be the free stream stagnation temperature but instead some fraction of that temperature. In order to better satisfy the physics of the situation, (1) will be rewritten as

$$(2) \quad i^2 R = h 2 \pi r \ell (T - T_e) \quad .$$

The recovery temperature,  $T_e$ , is the temperature of the wire at zero current. In terms of the Nusselt number, (2) is

$$(3) \quad i^2 R = \pi \ell k_e N (T - T_e) \quad .$$

Again by arguments of the physical situation the thermal conductivity,  $k_e$ , is based on the recovery temperature.

#### Cylinder With Conduction Loss

For the above situation with added conduction losses, the form of the equation remains approximately the same by the following argument developed by Demetriades [7]. The heat balance is now

$$(4) \quad i^2 R = \pi \ell k_e N (T - T_e) + L_C \quad .$$

The added conduction loss term,  $L_C$ , must be roughly proportional to the thermal conductivity of the wire,  $k_w$ , the temperature difference between the wire and the support,  $(T - T_s)$ , and the wire cross sectional area. It must also be roughly inversely proportional to the length,  $\ell$ , of the wire. Combining these arguments gives

$$(5) \quad L_C = C_1 \frac{\pi d^2 k_w}{4 \ell} (T - T_s) \quad , \quad C_1 = \text{constant} \quad .$$

Since the supports are many times larger than the wire and are wetted by the flow at temperature  $T_e$ , the supports can be assumed to be approximately at the recovery temperature also (lack of knowing the actual temperature leads the experimentalist to make some kind of assumption and the one assumed here is as appropriate as any). Equation (4) can now be written as

$$(6) \quad i^2 R = \pi \ell k_e N (T - T_e) + C_1 \frac{\pi d^2 k_w}{4 \ell} (T - T_e) .$$

This new conduction term can now be absorbed into a new Nusselt number which will include both conduction and convection losses so that

$$(7) \quad i^2 R = \pi \ell k_e N m (T - T_e)$$

where

$$(8) \quad Nm = N + \left( \frac{d^2}{\ell^2} \frac{C_1}{4} \frac{k_w}{k_e} \right)$$

or

$$(9) \quad Nm = N \left( 1 + \frac{C}{S^2} \right) , \quad S^2 = \frac{\ell^2}{d^2} \frac{k_e}{k_w} N .$$

If the term appearing in parenthesis in (8) or (9) is large then the conduction term is significant.

Kovaszny [11] and Dewey [12] have performed a more detailed calculation of the end losses. Their results are

$$(10) \quad Nm = N / \psi(S)$$

where  $\psi(S)$  is the correction. The dimensional argument indicates that  $S$  depends on the Nusselt number and the temperature loading. Therefore (10) can be written as

$$(11) \quad Nm = \frac{N}{f(N, \tau)} = Nm(N, \tau)$$



or

$$(12) \quad i^2 R = \pi \ell k_e N m(N, \tau) (T - T_e) \quad .$$

Kovaszny [11] and Dewey [12] give the exact solution as

$$(13) \quad \psi(S) = 1 - \frac{\tanh S}{S} \quad .$$

By comparing the exact solution given by (13) to the approximate solution given by (9) Demetriades [7] gives

$$(14) \quad \psi(S) = \frac{1}{1 + \frac{C}{S^2}} \quad .$$

This is satisfactorily close to (13) if the constant  $C$  is about four according to Demetriades [7].

#### Film Anemometer With No Substrate

For an electrically heated film with negligible radiation losses (see Appendix A) and no conduction losses the heat balance is

$$(15) \quad i^2 R = h A_S (T - T_e)$$

or, in terms of the Nusselt number,

$$(16) \quad i^2 R = k_e N A_S / w (T - T_e) \quad .$$

For the "homemade" films used, the area and characteristic length are not physically defined well enough to measure with acceptable accuracy. To accommodate this difficulty a new dimensional Nusselt number is defined as

$$(17) \quad N' = N A_S / w$$

so that (16) is now

$$(18) \quad i^2 R = k_e N' (T - T_e) \quad .$$

### Film Anemometer With Substrate

Assuming that the heat balance equation is of the same form as (18), the heat balance can be written

$$(19) \quad i^2 R = k_e N' (T - T_e) + L_C \quad .$$

Using the same argument as that used for the wire the conduction loss can be written as

$$(20) \quad L_C = C k_s \frac{A_s}{L} (T - T_e) \quad .$$

Yet another Nusselt number will be defined that is dimensional and includes both conduction and convection losses as

$$(21) \quad Nm' = N' + C_1 \frac{k_s}{k_e} \frac{A_s}{L} \quad .$$

Equation (19) can now be written in the form of convection losses only as shown in the following equation:

$$(22) \quad i^2 R = k_e Nm' (T - T_e) \quad .$$

It is known analytically and experimentally that the heat loss due to conduction to the supports is quite small for wires. Experimental results have shown that this is not so for films. In order to look more closely at this heat loss, a "thin-rod" model of the heat loss to the substrate will be examined. Figure 1

shows this model. This model assumes a constant cross sectional area and a constant thermal conductivity. It also assumes that the only temperature gradient is along the axis (no radial temperature distribution), that the face is held at a constant temperature, that the cylinder approaches the surrounding temperature as it extends to infinity, and that the surrounding temperature is the recovery temperature of the film. The differential equation describing the heat loss is

$$(23) \quad \frac{d^2 T}{dx^2} - \frac{h_B P}{k_S A} (T - T_e) = 0$$

where

$h_B$  = heat transfer coefficient for probe body

$P$  = perimeter of probe body

$k_S$  = thermal conductivity of substrate

$A$  = body cross sectional area .

Solving this equation gives the temperature distribution as

$$(24) \quad T = T_e + (T_f - T_e) e^{-\sqrt{\frac{h_B P}{k_S A}} x}$$

For a circular rod this may be written as

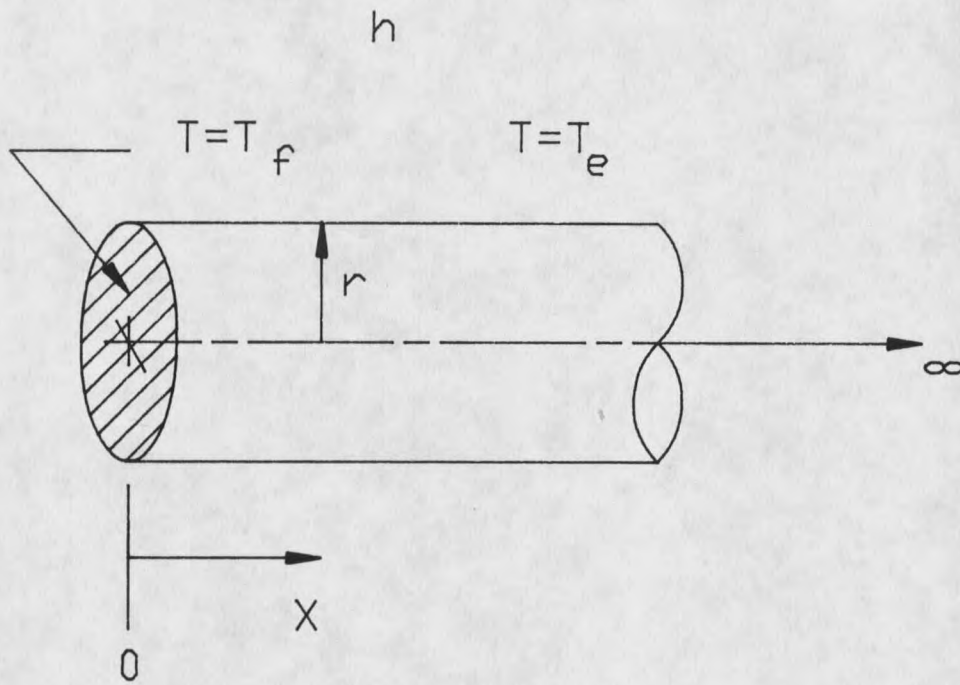
$$(25) \quad T = T_e + (T_f - T_e) e^{-\sqrt{\frac{2h_B}{k_S r}} x}$$

From (25)  $L$  in (21) can be approximated by taking the slope at  $x = 0$  of (25) and extending a line formed by this slope to the point where the temperature is equal to the fluid temperature as in Figure 2. If this is done it is found that

$$(26) \quad L = \sqrt{\frac{k_S r}{2h_B}}$$

or in terms of the Nusselt number of the rod near the film

$$(27) \quad L = r \sqrt{\frac{k_S}{k_e} \frac{1}{2N_B}}$$



B.C.

$$\begin{aligned} \text{At } x=0 \quad T &= T_f \\ \text{As } x \rightarrow \infty \quad T &\rightarrow T_e \\ A &= \text{constant} \\ k_s &= \text{constant} \end{aligned}$$

Figure 1. One-Dimensional Model for Heat Loss to Substrate.

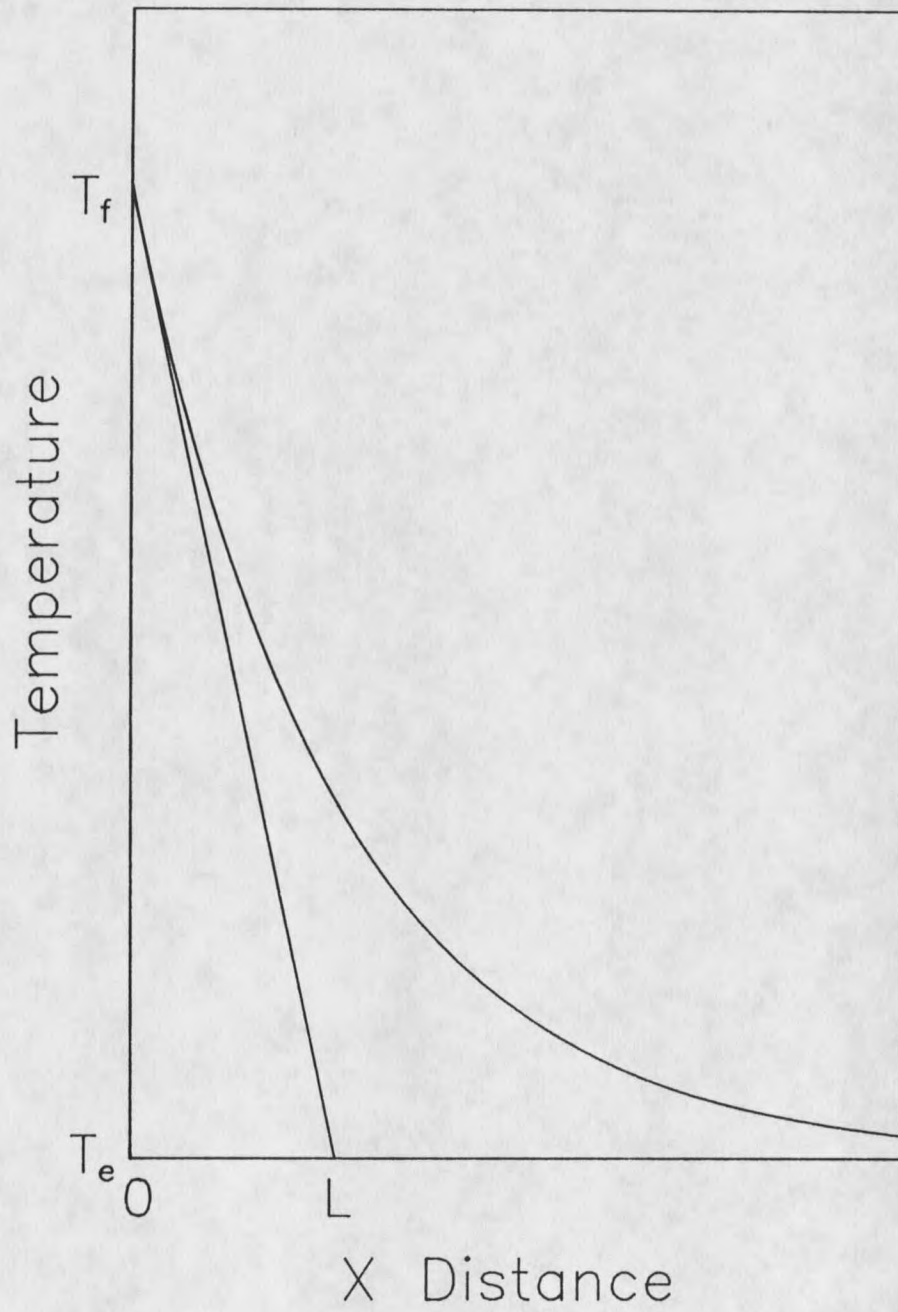


Figure 2. Approximation of Distance  $L$  for "Thin-Rod" Model.

Substituting (27) into (21) gives

$$(28) \quad Nm' = N' + C_1 \frac{A_f}{r} \sqrt{\frac{k_s}{k_e}} 2N_B$$

This equation says that for a low conduction loss the thermal conductivity of the substrate must be minimized. It can also be seen that since the thermal conductivity of the air is temperature dependent, the conduction loss term will also be temperature dependent. The thermal conductivity of the substrate material may also be temperature dependent. This dependence can not easily be found since the substrate can come in a truly infinite number of compositions and therefore tabulated data is likely unavailable. It is known by looking at [13] that some glasses vary as much as 10% in conductivity in the temperature range from zero to 100 C and that the amount by which the thermal conductivity changes will depend on the particular temperature range investigated. All other terms in (28) affect the convection loss as well as the conduction loss. The magnitude of these effects cannot be determined easily theoretically. It is known experimentally that this conduction loss term can amount to over 50% of the magnitude of the measured Nusselt number,  $Nm'$ , for Reynolds numbers ranging up to 100,000 1/cm.

Unfortunately the variable found from experiment is the measured Nusselt number,  $Nm'$ , in (28) which is dimensional and includes conduction effects. The variable of interest however is the convective Nusselt number,  $N$ . In order to extract this variable from the measured quantity additional work has to be done when reducing the data. This will be described later in Chapter 4.

#### General Heat Balance Equation

Regardless of the sensors examined or the boundary conditions applied, all of the heat balance equations developed so far have had the same general form. By

examining equations (3), (7), (18) and (22) it can be seen that the general form is

$$(29) \quad i^2 R = k_e \bar{N} (T - T_e)$$

where  $\bar{N}$  may include dimensions or conduction losses and is a function of Mach number, Reynolds number, and Temperature Loading (power). For films,  $\bar{N}$ , is dimensional and includes conduction losses. This general heat balance equation was originally noted by Demetriades [7].

## CHAPTER 4

## THEORY OF MEASUREMENT

From the theory of heat transfer from a film anemometer, the measured Nusselt number can be found by (22):

$$(30) \quad Nm' = \frac{i^2 R}{k_e (T - T_e)}$$

This expression is not nearly as simple as it first appears. The Nusselt number cannot be determined for the following reasons:

1. The recovery temperature,  $T_e$ , is not known.
2. Since the thermal conductivity is a function of the recovery temperature it is also an unknown.
3. The value of the measured Nusselt number,  $Nm'$ , is known through experimental work to be a function of power.
4. The Nusselt number found includes both convection and conduction effects (it is desired to find the "real" Nusselt number which includes convection effects only).

#### Resistance-Temperature Relations

In order to determine the recovery temperature, a relation between the resistance of the film and the surrounding temperature must be known. It is known that (reference [14]) resistance type sensors can be described by

$$(31) \quad R = R_r (1 + \alpha(T - T_r) + \beta(T - T_r)^2 + \xi(T - T_r)^3 + \dots)$$



For the film anemometer probes studied for the targeted temperature range this equation does not include terms past the quadratic. The number of terms retained is effected by the operation range of the instrument and its physical properties. For instance, hot-wires were typically operated from 10–200 C and used a linear fit but the films here were targeted for 10–760 C where a linear fit was found inadequate, as will be shown in Chapter 8. This will give the resistance at the recovery temperature as

$$(32) \quad R_e = R_r (1 + \alpha(T_e - T_r) + \beta(T_e - T_r)^2) \quad .$$

The recovery temperature can now be found if the reference resistance,  $R_r$ , the resistivity coefficients,  $\alpha$  and  $\beta$ , and the resistance at zero current,  $R_e$ , in the above equation are known. The equation will yield two solutions for the recovery temperature, only one of which will make sense physically. From (32) the recovery temperature is

$$(33) \quad T_e = \frac{-\alpha + \sqrt{\alpha^2 + 4\beta(R_e/R_r - 1)}}{2\beta} + T_r \quad .$$

As mentioned above, in order to determine the recovery temperature the reference resistance and the resistivity coefficients,  $\alpha$  and  $\beta$ , must be determined. This is done by performing an “oven calibration”. This calibration is done by finding the resistance at zero current for each known film temperature over a range of temperatures (see Chapter 7 for further detail on oven calibration procedures). The resulting set of resistance-temperature points can then be approximated by a second degree polynomial to obtain the coefficients in (32). Making the measurements of this needed resistance at zero current for each known temperature requires additional procedures. Points must be collected over a range of different powers and the resulting resistance versus power data fit to a second degree

polynomial as in Figure 3. This fit is then used to extrapolate to zero power to find the resistance at zero current. A second degree polynomial fit is chosen as the correct form of the relation by examining the theory of the dependence of the measured Nusselt number on power and by previous experimental results, as will be shown next.

### Nusselt Number Dependence On Power

The dependence of the measured Nusselt number on power cannot be determined directly from theory but it is known that such a dependence exists by looking at past experimental work. A simple relation will be assumed by expanding one over the measured Nusselt number in a Taylor series expansion and retaining only the first two terms, which is sufficient according to Demetriades [7]:

$$(34) \quad \frac{1}{Nm'} = \frac{1}{Nm'_e} - \frac{1}{Nm'^2_e} \left( \frac{\partial Nm'}{\partial W} \right)_e W ; \left( \frac{\partial Nm'}{\partial W} \right)_e = \text{constant}$$

After manipulation of (30), (32), and (34) and then letting the reference temperature be 0 C it can be found that

$$(35) \quad \begin{aligned} R = R_e + W & \left[ \frac{\alpha R_r}{k_e Nm'_e} + \frac{R_r 2\beta T_e}{k_e Nm'_e} \right] \\ & - CW^2 \left[ \frac{\alpha R_r}{k_e Nm'_e} + \frac{R_r 2\beta T_e}{k_e Nm'_e} - \frac{R_r \beta}{Ck_e^2 Nm'^2_e} \right] \\ & - C^2 W^3 \left[ \frac{R_r \beta 2}{Ck_e^2 Nm'^2_e} \right] + C_3 W^4 \left[ \frac{R_r \beta}{k_e^2 C Nm'^2_e} \right] \end{aligned}$$

where

$$(36) \quad C = \frac{1}{Nm'_e} \left( \frac{\partial Nm'}{\partial W} \right)_e$$

Equation (35) is in the following form:

$$(37) \quad R = R_e + AW + BW^2 + EW^3 + FW^4$$

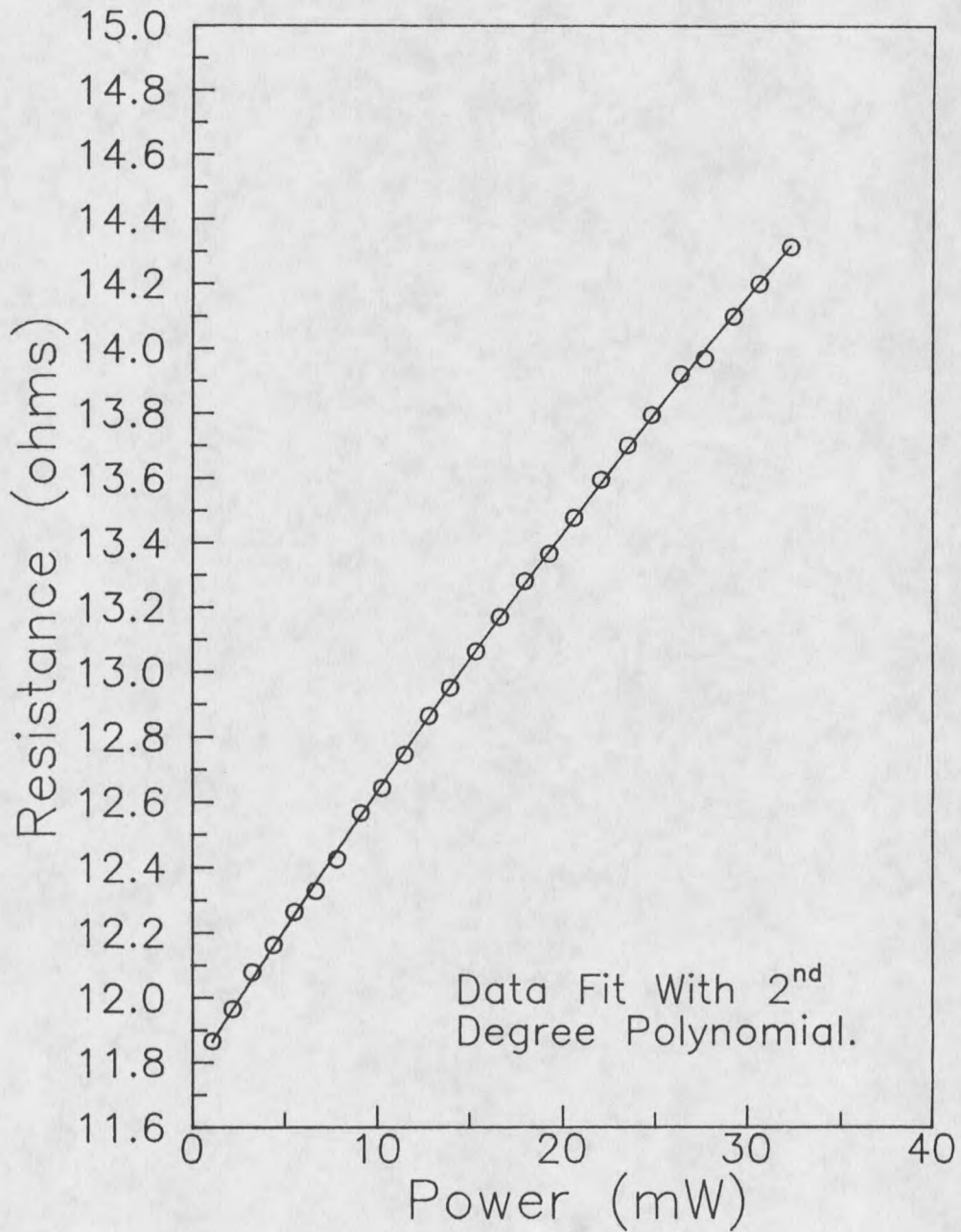


Figure 3. Film Resistance Dependence on Power Fit with a Second Degree Polynomial.

Equations (35) and (37) indicate that if the resistance versus power data are fit to a fourth order polynomial the measured Nusselt number at zero current can be found by relating the constant  $A$  in (37) to the corresponding term in (35) so that

$$(38) \quad Nm'_e = \frac{\alpha R_r}{Ak_e} \left( 1 + \frac{2\beta T_e}{\alpha} \right)$$

However, it is known experimentally that the coefficients  $E$  and  $F$  in (37) are close to zero, making a second degree polynomial fit sufficient. In (38) all variables can now be determined. The recovery temperature is now known from (33). The thermal conductivity can be found knowing the recovery temperature by using a textbook relation such as found in Irvine and Liley [15]. The resistivity coefficients and the reference resistance can be found by performing an oven calibration and finally, by making a second degree fit of the power versus resistance data the variable  $A$  can be determined. This will give the measured Nusselt number at zero current which still needs to be corrected so that the Nusselt number which is controlled only by convection can be found.

The Nusselt number dependence on power can more easily be examined if (35) is put in non-dimensional form. Since the coefficients  $E$  and  $F$  are zero, (35) can be written more simply as

$$(39) \quad R = R_e + W \left[ \frac{\alpha R_r}{k_e Nm'_e} + \frac{R_r 2\beta T_e}{k_e Nm'_e} \right] + CW^2 \left[ \frac{\alpha R_r}{k_e Nm'_e} + \frac{R_r 2\beta T_e}{k_e Nm'_e} - \frac{R_r \beta}{Ck_e^2 Nm_e'^2} \right]$$

Rewriting (39) in the form of (37) gives

$$(40) \quad R = R_e + AW + BW^2$$

where

$$(41) \quad B = C \left[ \frac{\alpha R_r}{k_e Nm'_e} + \frac{R_r^2 \beta T_e}{k_e Nm'_e} - \frac{R_r \beta}{Ck_e^2 Nm_e'^2} \right]$$

Now let

$$(42) \quad G = \frac{B}{C}$$

and

$$(43) \quad r = \frac{R - R_e}{R_e}$$

Substituting the above three equations into (39) will yield

$$(44) \quad r = \frac{AW}{R_e} + \frac{A^2}{A^2} \frac{R_e}{R_e} B \frac{W^2}{R_e}$$

Let

$$(45) \quad i_C^2 = 1/A$$

and

$$(46) \quad w = W/W_C ; \quad W_C = i_C^2 R_e$$

so that

$$(47) \quad r = w - \frac{BR_e}{A^2} w^2 = w - \frac{CGR_e}{A^2} w^2$$

Substitute (36) into (47):

$$(48) \quad r = w - \frac{G}{A^2} R_e \frac{1}{Nm'_e} \left( \frac{2Nm'}{2W} \right)_e w^2$$

Define a new variable  $D$  as

$$(49) \quad D = \frac{G}{A^2} \frac{R_e}{Nm'_e}$$

Equation (48) is now written as

$$(50) \quad r = w - Dw^2$$

According to (49) the constant  $D$  indicates how the Nusselt number depends on power. This can more easily be seen if, for purposes of clarity, the effect of the  $\beta$  term (from the oven calibration) on the Nusselt number dependence on power is assumed to be negligible. This simplifies (49) to

$$(51) \quad D = \frac{k_e R_e}{\alpha R_r} \left( \frac{\partial N m'}{\partial W} \right)_e$$

Though (51) is not the true definition of the constant  $D$  it draws the same conclusion as (49) and can more easily be understood. By looking at (50) it can be seen that the constant  $D$  can simply be found by curve-fitting the non-dimensional power versus resistance points and extracting the second coefficient. The value of  $D$  found will indicate the dimensional Nusselt number dependence on power. A value of zero would indicate no dependence and a value different than zero would indicate the magnitude of the dependence. The variables  $w$ ,  $r$ , and the constant  $D$  can also be used to determine if the number of terms in the Taylor Series expansion was sufficient by plotting  $(1 - r/w)/D$  versus  $w$ . Demetriades [7] has done this and concluded that the number of terms retained in the expansion is sufficient.

#### Conduction Term Correction

The loss due to conduction should be able to be determined experimentally despite theoretical difficulties if it is assumed that the loss is solely a function of the thermal conductivity of the surrounding fluid (see (28)). By theory it was determined that the conduction contribution to the measured Nusselt number depends linearly on the inverse square root of the thermal conductivity of the surrounding fluid (see (28)).

Since the thermal conductivity is a function of temperature the conduction contribution can also be written as a function of temperature. This temperature dependent conduction contribution will show up in the measured Nusselt number versus Reynolds number data. Each set of data taken at a different stagnation temperature will lie on its own line as shown hypothetically in Figure 4 by the symbolic squares and circles on the graph. By taking the data found for the relation between the measured Nusselt number and Reynolds number for each set and extrapolating to zero Reynolds number a measured Nusselt number without a convection term can be found for that particular set of data (labeled as  $N_{cnd1}$  and  $N_{cnd2}$  on Figure 4). The resulting extrapolated value should approximately include only conduction losses. This method assumes that the Nusselt number will be zero at zero Reynolds number. This is not strictly true due to natural convection currents. Given a different extrapolated measured Nusselt number for each stagnation temperature over a range of temperatures, a relation that connects the conduction loss to the fluid temperature can be found. Each conduction loss can then be subtracted from its corresponding set of measured Nusselt number - Reynolds number points so that the resulting data would be as in Figure 5 where the Nusselt number is now the desired variable of interest. Unfortunately extensive Nusselt number - Reynolds number data may not be available, and were not available for the measurements made in this study, for a large number of different temperatures. The alternative solution would be to use the oven calibration data. For each point taken during the oven calibration there is a corresponding Nusselt number at that temperature. This can be estimated as the measured Nusselt number at zero Reynolds number (referred to as the extrapolated measured Nusselt number above) by neglecting convection currents (see Appendix B). Assuming the absence of convection and radiation leaves conduction to be the only contribution

to the measured Nusselt number in the enclosed oven chamber. By using the oven calibration data this way a relation that connects the conduction contribution of the measured Nusselt number to the surrounding temperature can be found. This conduction contribution can then be subtracted from the measured Nusselt number found in a flow so that the convection Nusselt number can be obtained, which is the desired parameter. The results of this procedure should be as shown in Figure 5.

Much effort has been expended in arriving at the convective Nusselt number. This Nusselt number is the variable through which the heat transfer characteristics will be studied, which is the desired point of investigation.



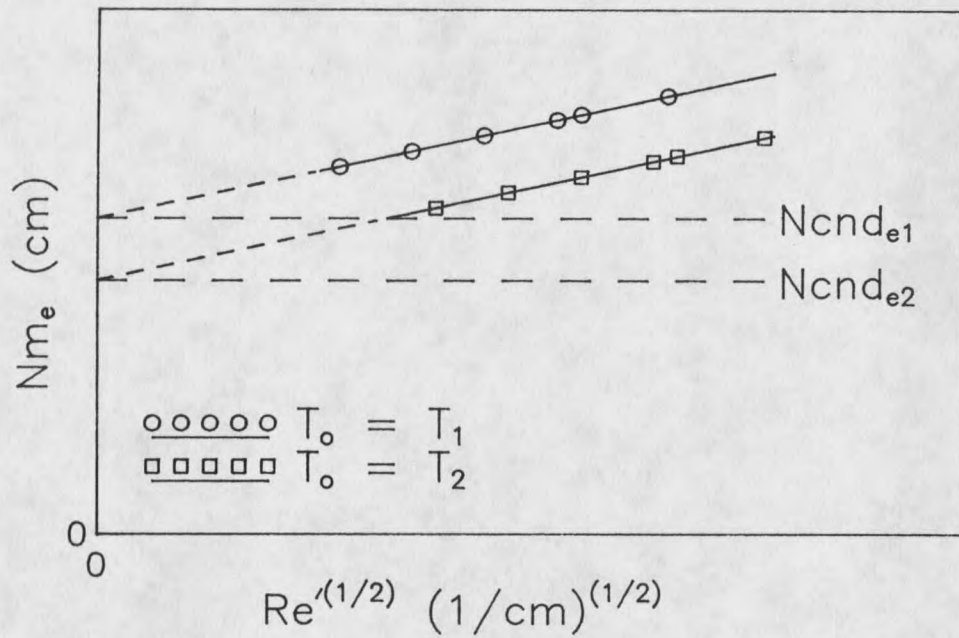


Figure 4. Hypothetical Case of Measured Nusselt Number Dependence on Flow Properties.

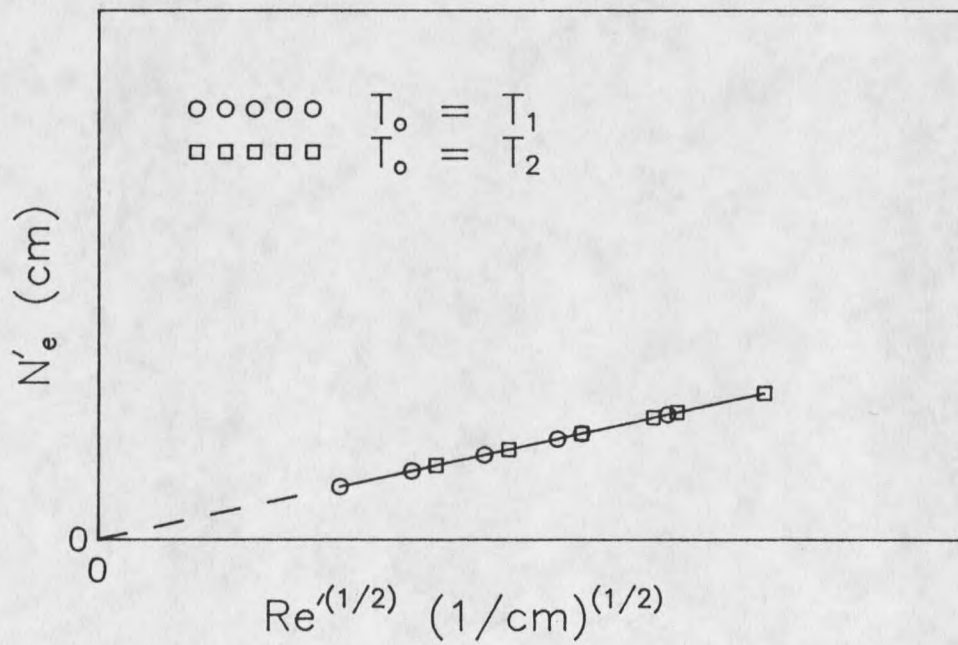


Figure 5. Hypothetical Case of "Actual" Nusselt Number Dependence on Flow Properties.

## CHAPTER 5

## HEAT TRANSFER FROM STAGNATION POINT SENSORS

Determining the Nusselt number is of no use unless it is somehow related to the flow characteristics. This is done by examining the heat transfer from stagnation point sensors and then drawing from hot-wire theory.

The local heat transfer rate of a sensor immersed in a flow is generally the highest at the stagnation line (Dewey [12], Sandborn [16], White [17]). Figure 6, originally presented by White [17], shows the local heat transfer rate from the surface of a hemisphere in a hypersonic laminar flow where  $q_w(0)$  is the heat transfer at the stagnation line. The correlation shown agrees closely with experimental data [17]. Figure 6 clearly shows that the heat transfer rate is the greatest at the stagnation line as compared to the other positions investigated.

This conclusion can also be arrived at by examining the fact that the driving parameter for heat transfer is the temperature gradient between the heat transfer surface and the surrounding flow. This gradient depends heavily on the boundary layer thickness which is thinnest at the stagnation line, resulting in the highest gradient in this region [19]. Since a higher gradient results in a higher heat transfer rate one would expect that the heat transfer rate would be the greatest at the stagnation line.

From this conclusion it can be said that hot-wires exchange much of their total heat transferred at the stagnation line. Similarly, since films are deposited on the stagnation line, the film anemometer heat transfer theory should conform

closely with that of the hot-wire heat transfer theory; the theory which connects the Nusselt number to the various flow parameters such as the Reynolds number, Grashof number, Mach number, the temperature loading, etc. as follows [10]:

$$(52) \quad N = N(Re, M, G, Pr, \tau, \dots)$$

Note that only forced convection is being considered. Also, for air in the range considered the Prandtl number will be taken as constant. This simplifies the above expression so that

$$(53) \quad N = N(Re, M, \tau)$$

This relation is shown by Dewey [12] in Figure 7. This figure indicates that the Nusselt number depends on Mach number for low Reynolds numbers where free-molecular effects are important [12]. From this and the previous conclusions regarding the similarities between film anemometers and hot-wires, film anemometers should follow the same general trends as found for hot-wires. The primary difference being that, since the hot-films are physically much larger than the hot-wires, the Reynolds number range shown in Figure 7 will be displaced to the right into the higher Reynolds number range for the hot-films. This would be of great advantage as it will eliminate the Mach number dependence of the Nusselt number on the Reynolds number. It is also expected that hot-films will show a Nusselt number dependence on the square root of the Reynolds number as is given by Kings Law [11] and as is found for hot-wires in the high Reynolds number range ( $Re > 20$ ) ([12],[20]).

In addition to knowing the hot-wire and film Nusselt number dependence on the Reynolds number, it is also required to know the temperature recovery factor dependence on the Reynolds number before either instrument can be used

as a tool for measuring flow properties. Comparisons of hot-wires and hot-films are difficult here due to the effects of the different geometries and supporting methods of each type of sensor. It can only be predicted that the temperature recovery factor should be one at Mach number zero and remain fairly close to one (within about 10%) as the Mach number varies. Exact values can be found only by experiment since they will depend, at a minimum, on individual probe geometry and supporting method.







































































































































































































































